J Sol-Gel Sci Technol (2010) 53:412–417
DOI 10.1007/s10971-009-2113-0

ORIGINAL PAPER

Effect of sulphate groups on catalytic properties of chromium supported by zirconia in the *n*-hexane aromatization

Sahar Raissi · Mohamed Kadri Younes · Abdelhamid Ghorbel · François Garin

Received: 12 August 2009 / Accepted: 7 November 2009 / Published online: 1 December 2009
© Springer Science+Business Media, LLC 2009

Abstract Catalysts based on chromium supported by sulphated and unsulphated zirconia have been synthesised, in one step, by sol–gel method and dried in hypercritical solvent conditions. Comparative study of their catalytic properties shows that dispersed Cr^{3+} seems to be the active species in the *n*-hexane aromatisation reaction. However, the acidity generated by sulphate groups acts as coke eliminator of the layers deposed on the surface mainly when catalyst is calcined at high temperature.

Keywords Aromatization · Zirconia · Chromium · Sol–gel

1 Introduction

The dehydrocyclization of light alkanes is one of the most attracting industrial operations that valorise light naphtha. It assures the increase of their octane number and allows, by consequence, their use as fuels [1]. The pathway reaction of *n*-hexane conversion may be explained by either mono or bi-functional mechanism [2, 3]. In the first case, a step of dehydrogenation followed by a ring closure and vice versa took place [2]. In the second case, *n*-hexane can be cracked and oligomerised on acid sites and then dehydrocyclization takes place on metallic sites [3].

Many transition metal oxides, particularly chromium oxides are applied in such processes [4]. In fact, chromia clusters and isolated Cr^{3+} ions seem to be active sites for such reaction involving dehydrogenation, oligomerisation and ring closure [4]. Pure and modified zirconia doped with metals (Pt, Cr) and prepared by impregnation method, have also attracted many interests [2–4]. This material is considered as an efficient system for aromatisation's reactions because of its exceptional redox and acid–base properties [5].

In this work, chromium supported on sulphated and unsulphated zirconia catalysts were elaborated by sol–gel method in one step with hypercritical solvent evacuation's conditions. The use of this method procures to solids very interesting characteristics. In particular, it offers a well dispersion of the metal on the supports lattice. The support acidity seems also to have some effects on the metal activity and mainly stability.

2 Experiments

The chromium catalysts supported on sulphated and unsulphated zirconia were prepared following the sol–gel procedure described by Mejri and al. [6]. The propoxide of zirconium (ALDRICH, 70% in propanol) is dissolved in propanol (ACROS 99%) to have a concentration of zirconium equal to 1 M. Then, the sulphate groups were introduced from concentrated sulphuric acid (ACROS 96%) with a molar atomic ratio $n\mathrm{S}/n\mathrm{Zr} = 0.5$ for the preparation of sulphated solids. Finally, the chromium acetylacetonate (ACROS 97%) was added with a proportion $n\mathrm{Cr}/n\mathrm{Zr}$ equal to 0.1. To form the alcogel, pure water was added with a

S. Raissi (✉) · M. K. Younes · A. Ghorbel
Laboratoire de Chimie des Matériaux et Catalyse, Département de Chimie, Faculté des Sciences de Tunis, 2092 El Manar Tunis, Tunisia
e-mail: r.sahar@hotmail.fr

F. Garin
Laboratoire des Matériaux, Surfaces et Procédés Pour la Catalyse, UMR 7515 CNRS—ULP—ECPM, 25 rue Becquerel, 67087 Strasbourg, France

hydrolysis ratio $n(H_2O)/nZr = 3$. Once the gel is formed, it is dried in an autoclave under solvent supercritical conditions to provide the aerogel solids. The obtained solids were then heated under oxidising or reducing atmosphere at different temperatures in the range 400–700 °C.

The catalysts are designed as AZSCrT, when they are sulphated and as AZCrT when they are not, A aerogel, Z zirconia, S sulphate, Cr chromium and T calcinations temperatures.

Catalysts' textural characterisation was performed by a Micromeritics apparatus type ASAP 2000, derived by a computer type AST. Samples were first degassed for 4 h under vacuum at 200 °C. Fifty absorption and desorption isotherm points of N_2 were obtained from which the specific surface area and pore size distribution were determined, respectively by BET and BJH methods.

XRD patterns were recorded on an automatic Philips Panalytical diffractometer using CuKα radiation and nickel monochromator. The reticular distances calculated are compared to those given by the Joint Committee on Powder Diffraction Standards.

UV-visible spectra were recorded on a Perkin Elmer spectrophotometer type Instrument lambda 45 coupled to an integration sphere type RSA-PE-20 in the range 200–900 nm with a speed of 960 nm min^{-1} and an aperture of 4 nm.

XPS spectra were obtained using a VG Escalab 220XL spectrometer. The source was monochromatic AlKa radiation (1,486.6 eV; 100 W) spot size of 500 μm diameter, electromagnetic mode for lens with pass energy of 30 eV and flood gun compensation were used C1s level of hydrocarbon contaminant was taken as the internal reference at 285, 0 eV.

Elemental analyses were performed by a "flash combustion" procedure using an Elementar Analyser EA Oriba jobin yvon type inea 220.

The *n*-hexane aromatisation reaction was carried out on 0.100 g sample in a tubular reactor operating at atmospheric pressure at 450 °C. Catalyst was put on contact with the feed gas diluted with Helium at a flow rate of 30 mL min^{-1} and inlet partial pressure of *n*-hexane of 10 Torr. The products were analysed with an on-line chromatogram and a FID detector. The catalysts were used either calcined under oxygen or after reduction treatment by H_2.

3 Results and discussion

As it appears on Fig. 1, sulphated and unsulphated aerogels develop a tetragonal ZrO_2 phase even before calcination. The stabilisation of this phase is always related to the effect of addition of sulphate groups to zirconia [6, 7]. On the other hand, chromium seems also to play an important role in the prevention of the transition tetragonal-monoclinic ZrO_2 phase [8]. Its role is mainly manifested at high calcination temperature, when a partial loss of sulphate occurs (Table 1).

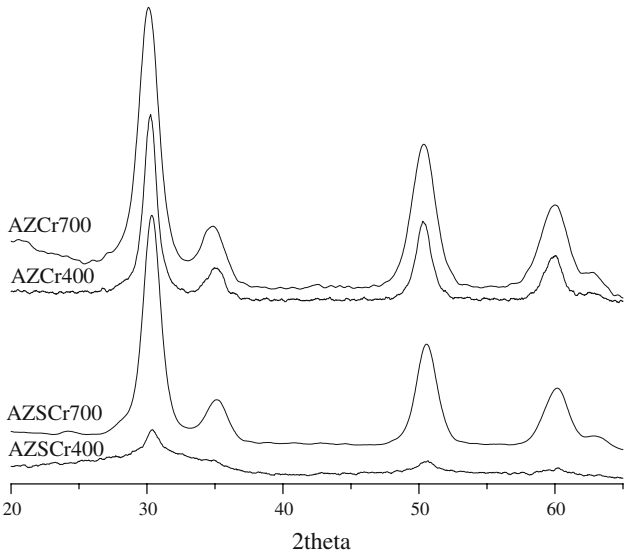

Fig. 1 DRX patterns of calcined catalysts: AZSCr400, AZSCr700, AZCr400, AZCr700

Moreover, the way of preparation of the catalysts and principally the drying under high pressure appears also as an influent factor for the stabilisation of this crystal phase as described later [6, 9].

However, no crystalline phase relative to any chromium oxide was detected which is probably due to either the low Cr content or a dispersion of this metal on the surface of zirconia [10, 11]. Even after the reducing treatment in a flow of H_2, the ZrO_2 tetragonal phase was not altered and no other crystalline phase was detected (Fig. 2).

The textural characterisation of the catalysts was evaluated from nitrogen adsorption–desorption isotherms and has revealed some differences between the sulphated and the unsulphated solids.

The sulphated catalysts calcined at different temperatures exhibiting the type IV isotherms with H3 hysteresis loop according to the IUPAC classification [13] (Fig. 3). Their textures are consequently mesoporous with tubular and cylindrical pores with a diameter around 140 Å (Fig. 4).

Whereas, the isotherms of the non sulphated catalysts appear as a superposition of type II and type IV isotherms characteristic, respectively of macroporous and mesoporous materials (Fig. 5). In fact, their corresponding BJH pore distribution show two types of pores (Fig. 6). The first is centred at 40 Å and the second is large and situated in the macroporous range.

Table 1 S_{BET} and sulphur contains of calcined and reduced catalysts

	AZSCrT				AZCr			
	Non reduced		Reduced		Non reduced		Reduced	
Calcination temperature T (K)	673	973	673	973	673	973	673	973
S_{BET} (m^2 g^{-1})	213	131	120	105	198	83	150	75
Sulphur contains (%)	3.84	0.71	0.61	0.45	–	–	–	–

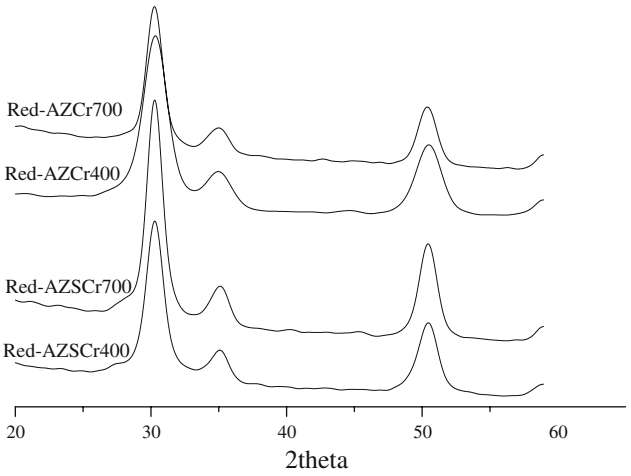

Fig. 2 DRX patterns of reduced catalysts: AZSCr400, AZSCr700, AZCr400, AZCr700

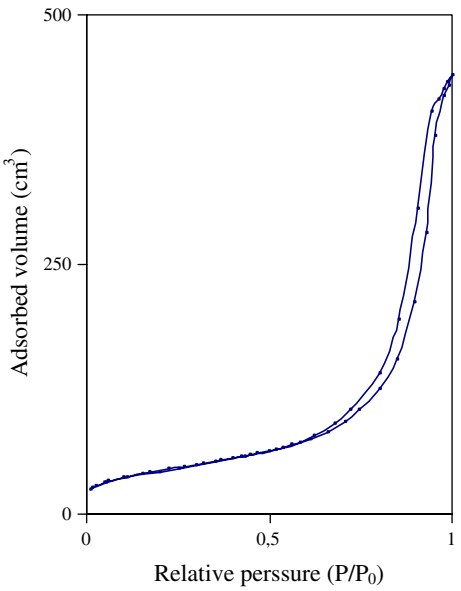

Fig. 3 Adsorption–desorption isotherm of N2 on sulphated catalysts

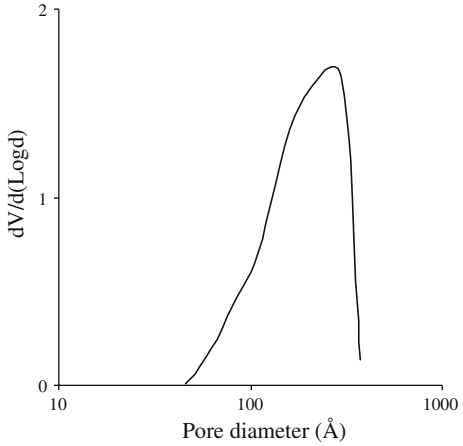

Fig. 4 Porous distribution of sulphated catalysts

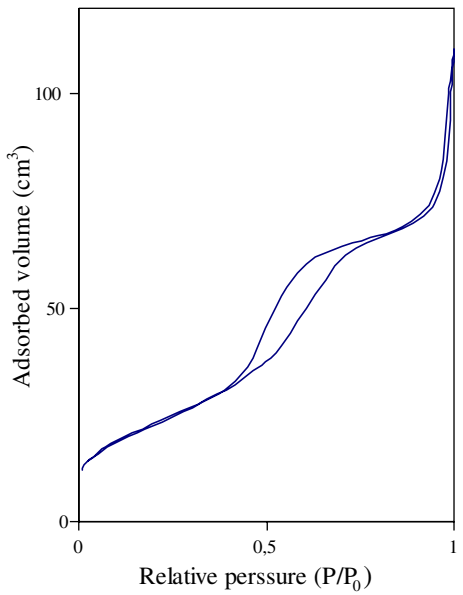

Fig. 5 Adsorption–desorption isotherm of N2 of unsulphated catalysts

A high temperature treatment under oxygen of the two kinds of solids causes a decrease of the S_{BET} as appears on Table 1 which is due to a phenomenon of sintering.

H_2 treatment of catalysts provokes also a decrease of the specific surface area that is more noticeable when the solids are firstly calcined at low temperature particularly for the sulphate doped solids. Indeed, this treatment causes an easy departure of sulphur. Besides, the reduction of the surface may be induced either by apparition of small crystallites or their sintering.

The UV-Visible spectra of all the aerogel catalysts heated under O_2 (Figs. 7, 8), are predominated by a group

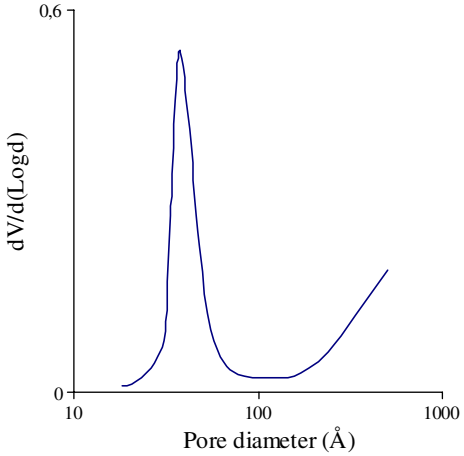

Fig. 6 Porous distribution of unsulphated catalysts

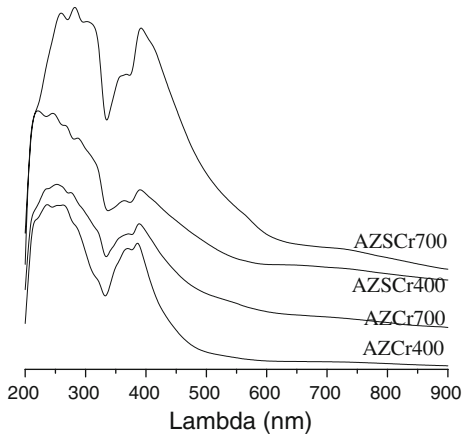

Fig. 7 UV-visible spectra of calcined catalysts: AZSCr400, AZSCr700, AZCr400, AZCr700

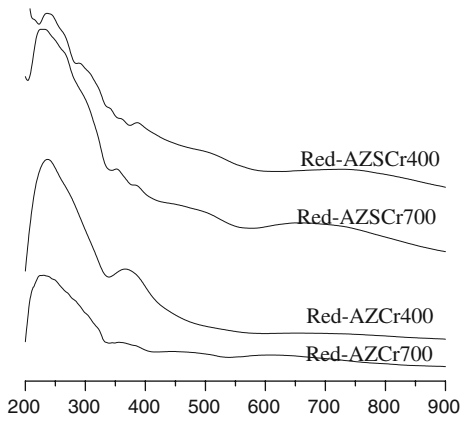

Fig. 8 UV-visible spectra of reduced catalysts: AZSCr400, AZSCr700, AZCr400, AZCr700

of bands situated at 260, 287, 320 and 380 nm attributed to $O^{2-} \rightarrow Cr^{6+}$ LMCT in monochromates and polychromates groups [14, 15]. The multiplicity of those bands reveals that Cr^{6+} is in different symmetry and/or with different length of the Cr–O bond [15, 16]. In addition we note the presence of two bands with a low intensity between 400–500 and 600–700 nm. These bands can be related to Cr^{3+} d–d transition in a small quantity of octahedral Cr^{3+} in an amorphous Cr_2O_3 or isolated Cr^{3+}ions on the surface of aerogel zirconia [11]. These species are more developed at high calcination temperatures and seems to be essentially due to the use of the sol–gel procedure that contributes to the formation of solids with nanometric size and in a particular state of division [12].

These results are in agreement with XPS study. As shown in the Fig. 9, chromium exists in the oxidation state III and VI for calcined catalysts. In fact, the Cr2p photopeak could be decomposed in two components centred around, respectively at 576 for Cr^{3+} ions and 5,787.4 eV for Cr^{6+} [17] Cr^{3+}/Cr^{6+} ratio in the surface is in the proportion 1.1 for the sample calcined at 400 °C however, it becomes 1.5 for the one calcined at 700 °C.

The introduction of sulphate groups seems to not affect the chromium oxidation state. However, it changes the zirconium coordinance. In fact, for sulphated catalysts the band relative to $O^{2-} \rightarrow Zr^{4+}$ LMCT is situated at 210 nm which implies that the tetragonal zirconia has a high coordinance. It is shifted to 228 nm for unsulphated catalysts which implies a decrease in the coordinance (probably to 7) [18].

The reductive treatment under H_2 induces a clear decrease in the intensity of the Cr(VI) bands and as a consequence an increase of the bands relative to Cr(III) in the two kinds of solids.

The catalytic results for the different solids are reported on Figs. 10 and 11. They reveal that all the catalysts are totally selective towards benzene. The absence of side products such as cracking and isomerisation products suggests that the reaction mechanism is monofunctional [2, 19, 20]. In fact, this mechanism consists on the formation of cyclic intermediate followed by its dehydrogenation which provides a high selectivity to the catalysts. However, bifunctional mechanism is renowned for its less important selectivity toward aromatics because it involves throw steps of skeletal changes like alkane isomerisation or C–C splitting which take place on acid sites [21]. Thus, the metallic function, which catalyses the dehydrogenation and 1, 6 ring closure, can be considered as the active site in our conditions using He as diluting gas. In fact, it has been shown that the absence of H_2 from the reaction mixture is not favorable for the occurrence of isomerisation and cracking processes [22].

The catalytic activity is improved for the high calcination temperatures and after heating under H_2 flow as reported on the Figs. 10 and 11. This result suggests that chromium in the oxidation state +3 seems to play a key

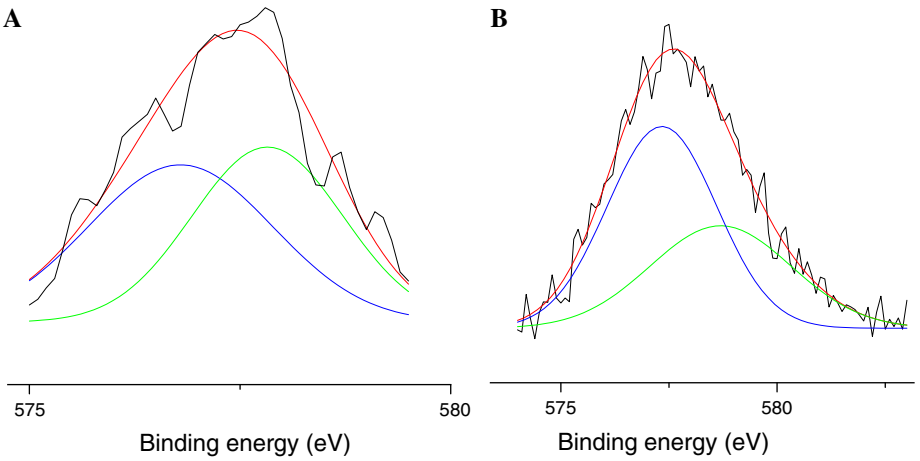

Fig. 9 XPS spectra of Cr2p of: **a** AZSCr400, **b** AZSCr700

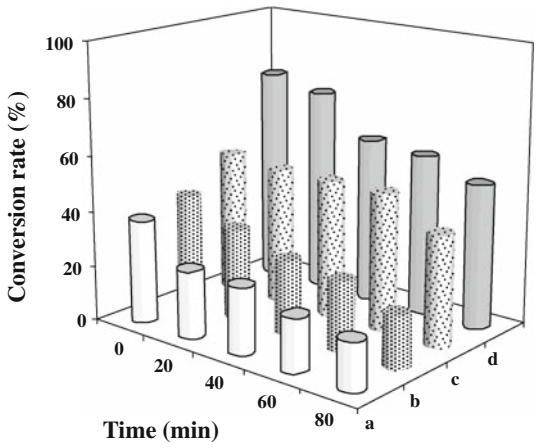

Fig. 10 Conversion rate of sulphated catalysts versus time: **a** AZSCr400, **b** AZSCr700, **c** reduced AZSCr400, **d** reduced AZSCr700

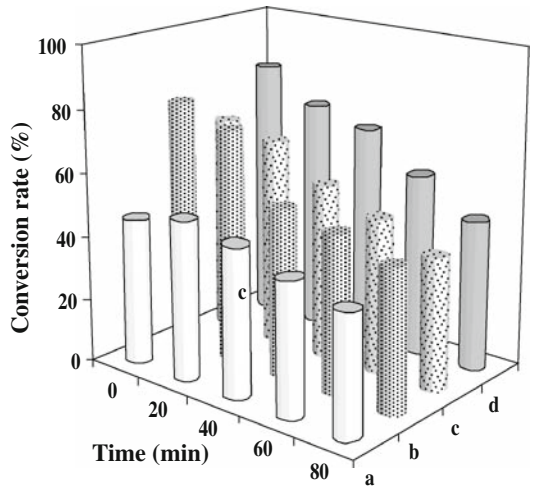

Fig. 11 Conversion rate of unsulphated catalysts versus time: **a** AZCr400, **b** AZCr700, **c** reduced AZCr400, **d** reduced AZCr700

role in the aromatization reaction as shown by the UV–visible and XPS study in which Cr^{3+} is favoured at high calcinations temperature and reductive treatment.

The introduction of sulphates in chromium supported by zirconia catalyst seems not to be of great interest in the amelioration of the catalytic properties. This is due to the fact that the reaction mechanism is monofunctional involving Cr^{3+} sites. However, it contributes to the stabilisation of catalysts. Indeed, the functionality loss is less noticeable in presence of sulphate groups responsible of the generation of more acid sites [23, 24]. This can be explained by an aptitude of such solids, thinks to their acid properties, to remove the coke [5].

Moreover, it is important to note that under reducing conditions at high temperature, Zr^{3+} could be formed on the surface of zirconia [5]. This species is also thought to constitute active site for aromatisation as it is reported by Hoang and al. [5, 25].

4 Conclusion

The *n*-hexane aromatisation reaction carried out on the chromium sulphated and unsulphated zirconia needs Cr^{3+} species as active sites. Whereas sulphate groups introduced in catalyst does not develop this active species but can play an important role to stabilise catalyst.

References

1. Kumar M, Saxena AK, Negi BS, Viswanadham N (2008) Catal Today 130:501
2. Klepel O, Breitkopf C, Standke M (2004) J Mol Catal A 210:211
3. Mikhailov MN, Mishin IV, Kustov LM, Lapidus AL (2007) Micro Meso Mater 104:145
4. Gnep NS, Doyemet JY, Guisnet M (1988) J Mol Catal 101:281
5. Hoang DL, Farrage SA-F, Radnik J, Pohl M-M, Schneider M et al (2007) Appl Catal A 333:67
6. Méjri I, Younes MK, Ghorbel A (2006) J Sol–gel Sci Tech 40:3
7. Davids BH, Keagh RA, Srinivasan R (1994) Catal Today 20:219
8. Stefanic G, music S, Gajovic A (2005) J Mol Struct 744:541

9. He D, Zhao Q, Wang WH, Che RZ et al (2002) J Non-Cryst Solids 297:84
10. Yim SD, Nam I (2004) J Catal 221:601
11. Gaspar AB, Dieguez LC (2003) J Catal 220:309
12. Bedilo AF, Klabunde KJ (1997) Nano Struct Mater 8:119
13. IUPAC recommendations (1994) Pure Appl Chem 66:1739
14. Fuijdala LK, Tilly TD (2003) J Catal 218:123
15. Younes MK, Ghorbel A, Naccache C (1997) J Phys Chem 94:1993
16. Ellison Q, Oubridge JOV, Sing KSW (1970) J Chem Soc Faraday Trans 66:1004
17. Deng S, Li H, Li S, Zhang Y (2007) J Mol Catal A 268:169
18. Castellon ER, Lopez AJ, Torres PM (2003) J Solid State Chem 175:159
19. Smiešková A, Rojasová E, Hudec P, Šabo L (2004) Appl Catal A 268:235
20. Trunschke A, Hoang DL, Radnik J, Brzezinka K-W et al (2001) Appl Catal A 208:381
21. Hoang DL, Preiss H, Parlitz B, Krumeich F et al (1999) Appl Catal A 182:385
22. Kim SY, Goodwin JG, Hammache S, Auroux A et al (2001) J Catal 201:1
23. Hua W, Sommer J (2002) Appl Catal A 227:279
24. Sakthivel R, Prescott HA, Deutsch J, Lieske H, Kemnitz E (2003) Appl Catal A 253:237
25. Hoang DL, Preiss H, Parlitz B, Krumeich F, Lieske H (1999) Appl Catal A 182:38